IEEE Access
Multidisciplinary ⋮ Rapid Review ⋮ Open Access Journal

Received 3 March 2023, accepted 15 March 2023, date of publication 24 March 2023, date of current version 29 March 2023.

*Digital Object Identifier 10.1109/ACCESS.2023.3261259*

RESEARCH ARTICLE

# Multi-Slope Path Loss Model-Based Performance Assessment of Heterogeneous Cellular Network in 5G

**SAFIA AMIR DAHRI[1], MUHAMMAD MUJTABA SHAIKH[1], MUSAED ALHUSSEIN[2], MUHAMMAD AFZAL SOOMRO[3], KHURSHEED AURANGZEB[2], (Senior Member, IEEE), AND MUHAMMAD IMRAN[4], (Member, IEEE)**

[1]Department of Telecommunication Engineering, Quaid-e-Awam University of Engineering, Science and Technology, Nawabshah 67450, Pakistan
[2]Department of Computer Engineering, College of Computer and Information Sciences, King Saud University, P. O. Box 51178, Riyadh 11543, Saudi Arabia
[3]Department of Mathematics and Statistics, Quaid-e-Awam University of Engineering, Science and Technology, Nawabshah 67450, Pakistan
[4]Institute of Innovation, Science and Sustainability, Federation University, Brisbane, VIC 4000, Australia

Corresponding authors: Khursheed Aurangzeb (kaurangzeb@ksu.edu.sa) and Safia Amir Dahri (engrsafia@quest.edu.pk)

This research was funded by Researchers Supporting Project number (RSPD2023R553), King Saud University, Riyadh, Saudi Arabia.

**ABSTRACT** The coverage and capacity required for fifth generation (5G) and beyond can be achieved using heterogeneous wireless networks. This exploration set up a limited number of user equipment (UEs) while taking into account the three-dimensional (3D) distance between UEs and base stations (BSs), multi-slope line of sight (LOS) and non-line of sight (n-LOS), idle mode capability (IMC), and third generation partnership projects (3GPP) path loss (PL) models. In the current work, we examine the relationship between the height and gain of the macro (M) and pico (P) base stations (BSs) antennas and the ratio of the density of the MBSs to the PBSs, indicated by the symbol $\beta$. Recent research demonstrates that the antenna height of PBSs should be kept to a minimum to get the best performance in terms of coverage and capacity for a 5G wireless network, whereas ASE smashes as $\beta$ crosses a specific value in 5G. We aim to address these issues and increased the performance of the 5G network by installing directional antennas at MBSs and omnidirectional antennas at Pico BSs while taking into consideration traditional antenna heights. The authors of this work used the multi-tier 3GPP PL model to take into account real-world scenarios and calculated SINR using average power. This study demonstrates that, when the multi-slope 3GPP PL model is used and directional antennas are installed at MBSs, coverage can be improved 10% and area spectral efficiency (ASE) can be improved 2.5 times over the course of the previous analysis. Similarly to this, the issue of an ASE crash after a base station density of 1000 has been resolved in this study.

**INDEX TERMS** HCN, multi-slope path loss model, IMC mode, 5G, area spectral efficiency.

## I. INTRODUCTION

Macro, micro, pico, and femtocells are only a few of the several network technologies that are combined in heterogeneous cellular networks (HetNets) to provide effective coverage and capacity for various locations and use cases. The main goal of HetNets is to optimize network performance by dynamically allocating network resources to satisfy the changing requirements of various devices and services. HetNets use a combination of different radio access technologies (RATs) and frequencies and employ advanced techniques such as load balancing, self-organization, and interference management to provide efficient and effective network operation. In addition, HetNets use small cells to supplement macro cells and provide increased capacity and coverage in stadiums, shopping centres, and urban centres are examples of high-density areas. The 3GPP is working to define the standards and protocols for HetNets, and there have already been a number of commercial HetNet deployments in various regions of the world. A work package for Release 18,

The associate editor coordinating the review of this manuscript and approving it for publication was Miguel López-Benítez.

which is billed as the first release of 5G Advanced and marks a significant advance, was approved by the 3GPP radio access network (RAN) plenary. The work package consists of various research and development tasks that will greatly improve 5G performance and address a wide range of novel use cases. The authors of [1] provide an overview of the development of 5G Advanced in 3GPP Release 18. HetNets is expected to play a key part in the development of 5G networks, and current research and development efforts are concentrated on enhancing HetNets' performance, effectiveness, and scalability to meet the rising demands of next-generation wireless networks.The adoption of smart gadgets has naturally increased demand for cellular network capacity and coverage. Everyone who uses a computer or mobile device has access to social media and several programmes, including WhatsApp, YouTube, Facebook, Twitter, Tiktok, Instagram, and many more. In order to address the epidemiological concerns, in [2], authors emphasise the evolving roles of 5G technology. Reference [2] also analyses several technological obstacles and the potential for creating healthcare applications powered by 5G. In [3] the Hamburg port in Germany was the area under investigation from 2020 to 2030. That findings demonstrate that there is a strong commercial case for a 5G network that offers upgraded mobile broadband services exclusively. Data and data rates are consumed continuously. Likewise, by deploying an increasing amount of small cells, commercial wireless networks are shifting towards higher frequency reuse in order to better handle traffic [4], [5]. The Shannon-Hartley theorem is a fundamental theorem in information theory that relates the maximum capacity of a communication channel to its bandwidth and the signal-to-noise ratio (SNR). Shannon law gives the following different methods for enhancing the capacity and coverage [6].

(1) Increasing bandwidth: The Shannon-Hartley theorem states that the maximum capacity of a communication channel is proportional to the bandwidth of the channel. Therefore, increasing the available bandwidth can increase the capacity of the system.
(2) Improving signal-to-noise ratio (SNR): The SNR is the ratio of the power of the signal to the power of the noise in the channel. Increasing the SNR by reducing noise and increasing signal power can increase the system's capacity.
(3) Using multiple access techniques: The number of users that can be supported in a communication system can be increased by using multiple access techniques like frequency division multiple access (FDMA), time division multiple access (TDMA), code division multiple access (CDMA), and orthogonal frequency division multiple access (OFDMA).
(4) Using advanced modulation schemes: Advanced modulation schemes such as quadrature amplitude modulation (QAM), phase shift keying (PSK), and amplitude shift keying (ASK) can increase the amount of data that can be transmitted over a given bandwidth.
(5) Using adaptive modulation and coding: Adaptive modulation and coding (AMC) techniques can adjust the modulation and coding schemes used based on the channel conditions, allowing for increased data rates and improved reliability.
(6) Using multiple-input multiple-output (MIMO) techniques: MIMO techniques use multiple antennas at the transmitter and receiver to increase the data rate and improve the reliability of the system.
(7) Using network topology optimization: Optimizing the topology of the network, including the placement of base stations, can improve the coverage and capacity of wireless networks.

It is worth noting that each of these techniques has its advantages and limitations, and the choice of technique depends on the specific requirements and constraints of the communication system. The most successful strategy, however, is to use BSs with varying powers because adding spectrum is the simplest but least expensive method. When a cellular network is heterogeneous, it can offer increased capacity, increased coverage, and high data transfer (macro, pico, or femto) [7], [8], [9]. Cellular networks become more difficult to analyse using traditional techniques as a result of heterogeneity. Furthermore, a heterogeneous cellular network can be examined by applying a particular probability distribution to each of its nodes [10], [11]. One analysis technique that models randomly distributed points is stochastic geometry [12]. In order to examine the 4G and 5G networks, a particular distribution called the Poisson point process (PPP) is used. The density of the network made possible by the frequency reuse concept has increased cellular networks' capacity and coverage during the past few years. It's anticipated that nothing will change for a long time. As a result, it became impossible to offer the required capacity and coverage due to the growing interference brought on by the same BSs. The increasingly popular 5G wireless network requires deployments that are both dense and diversified. The heterogeneous cellular network of 5G, which consists of a regular cellular network overlaid with various types of small cells, macro, pico, or femtocells, considerably aids in realising the requirement of a 100-fold increase in mobile network throughput compared to the already prevalent 4G one [13].

The structure of the paper is as follows: A review of the literature is included in section II. Part 3 of the document discusses the system model. Part 4 presents the performance metrics, while Section V elaborates on the findings and their justification. The study's result is then presented.

## II. LITERATURE REVIEW

The mobile capacity needed for 5G, the fifth generation of wireless communication, is 100 times greater than that needed for 4G. Co-channel deployment of macro cell base stations (MBSs) and small cell base stations (SBSs) using the same frequency spectrum can accomplish that. Reference [14], [15], and [16] have all received a lot

of attention recently. By arranging their nodes according to the homogeneous point Poisson process (HPPP), Andrews et al. [17], [18] analysed networks with BSs with the same power. They came to the conclusion that in interference-limited circumstances, the likelihood of coverage is independent of the density of the BSs, or $\lambda_{BSs}$. The likelihood of coverage is likewise independent of $\lambda_{BSs}$ for each BS in the network with BSs having varying powers, according to Dhillon et al analysis of the aforementioned [17]. On the other hand, Zhang and Andrews [19] demonstrated that the likelihood of coverage strongly depends on $\lambda_{BSs}$ by using the dual-slope path loss model. Using a multi-slope path loss model and the shortest path loss association criterion, Ding et al. [20] show that the probability of coverage initially rises with the $\lambda_{BSs}$ and then falls. Moreover, as the $\lambda_{BSs}$ rises, the area spectral efficiency (ASE) will grow practically linearly. A stretched exponential path loss model for short-range communication was put forth in [21]. They demonstrated for this reason that the ASE does not decrease with the $\lambda_{BSs}$ and that coverage is the same at large density. It is crucial to remember that the study cited above demonstrates that due to the infinite UEs, BSs would always be active and broadcast signals for all time. Of course, in actual use, especially in ultra-dense networks (UDNs), this may not be the case. Lee and Huang [22] first assume a network with BSs having the same power and finite number of UEs in order to analyse more realistic network performance. They next examined its likelihood of coverage and arrived at the best $\lambda_{BSs}$ in accordance. Furthermore, system-level analysis of cellular networks in [23] establishes the reliability of building tracks in densely populated metropolitan contexts as a function of blockages and $\lambda_{BSs}$. According to a traceable performance study presented in [24], the UEs and $\lambda_{BSs}$ have a strong correlation with the ASE's upward trend. Using probabilistic line-of-sight (LoS) and non-LoS (NLoS) transmissions, Ding et al. analysed the likelihood of coverage and ASE of a network with BSs of equal power. This network has limited UEs and pico cell BSs that are capable of operating in idle mode (IMC). According to the IMC, the BS will be powered off and no signal will be sent if there isn't an active UE present inside its coverage region. As a result, it is possible to increase the likelihood that UEs will be covered and the system's energy efficiency, which is inversely related to network density. While the interference power remains constant or even drops due to IMC, the UEs can receive stronger signals from the closer BSs. In contrast to the earlier findings in [17] and [25], the conclusion in [26] is that the probability of coverage relies on the $\lambda_{BSs}$ in an interference-limited network. New information was provided for the development of 5G networks. The authors of [27] examined the probability of coverage and came to the conclusion that the probability of coverage relies on antenna height at pico Base Stations (HP). Due to variability, these results diverge from [28] and [29]. Macrocells and pico/small cells, which differ in terms of transmission power and coverage area, make up the heterogeneous cellular network (HetNet) used by the authors for this study. This allows authors to effectively manage the radio resources in a certain area while improving coverage and capacity by utilising two BSs types, each with their own distinct properties. For instance, picocells can be used to offer coverage in highly populated areas where there is a strong demand for wireless connectivity, whereas macrocells can be utilised in rural areas where there is a lesser demand but a greater need for coverage. Furthermore, by offering more dependable and constant connectivity, HetNets can raise the quality of service (QoS) for users. With two types of BSs in the network, users can be dynamically switched between BSs based on their location and the level of traffic in the network. This can help to reduce congestion and ensure that users have a consistent level of service regardless of their location. In this study, authors are calculating SINR (Signal-to-Interference-plus-Noise Ratio) based on average power which has several advantages over calculating it based on instantaneous power, including:

1) More Stable Performance: In a heterogeneous cellular network, the signal power can vary significantly over time and space due to the presence of different cell types and varying signal strengths. Calculating SINR based on instantaneous power can result in unstable performance due to the rapid changes in the signal power. On the other hand, calculating SINR based on average power provides a more stable and reliable performance as it takes into account the average power of the signal over time and space.
2) Reduced Interference: Calculating SINR based on average power can help reduce interference in the network. This is because interference can vary significantly based on the instantaneous power of the interfering signals, which can result in higher interference levels and reduced SINR. By calculating SINR based on average power, the impact of interference is reduced, as it takes into account the average interference power across the network.
3) Simplified Network Management: Calculating SINR based on average power simplifies network management as it requires less frequent measurement and processing of instantaneous power levels. This is because calculating SINR based on instantaneous power requires frequent updates of power measurements, which can lead to increased complexity in network management.
4) Better Resource Allocation: Calculating SINR based on average power can improve resource allocation in the network. This is because it takes into account the average power of the signal and interference, which can be used to optimize resource allocation and avoid overloading certain cells with higher-power signals.

Hence, calculating SINR based on average power is a more stable, reliable, and simplified approach for heterogeneous cellular networks, which can help reduce interference,

simplify network management, and improve resource allocation. The authors have used 3GPP specified multi-slope path loss model which is a more accurate and realistic model for path loss model in a heterogeneous cellular network compared to the free space path loss model. Here are some advantages of using multi-slope path loss in a heterogeneous cellular network:

1) Better Model of Real World Environments: Multi-slope path loss takes into account the physical characteristics of the environment, such as terrain, buildings, and other obstructions that can affect the propagation of signals. This makes it a more realistic model for path loss in a heterogeneous cellular network compared to free space path loss, which assumes a clear line-of-sight path between the transmitter and receiver.
2) Enhanced User Experience: Using multi-slope path loss in a heterogeneous cellular network can improve the user experience by providing more accurate and reliable signal strength and coverage. This is because the multi-slope path loss model takes into account the physical environment, which can significantly affect signal propagation.

Overall, the authors have a more precise and realistic path loss model by using multi-slope path loss in a heterogeneous cellular network. The usage of three-dimensional distance (3D) by authors in place of two-dimensional distance (2D) has various benefits, including

1) More Accurate Path Loss Estimation: Using three-dimensional distance takes into account the vertical distance between the transmitter and receiver, which can significantly affect the path loss. In a heterogeneous cellular network, where cell types have varying heights, using three-dimensional distance provides a more accurate path loss estimation, leading to better signal coverage and improved network performance.
2) Improved Resource Allocation: Using three-dimensional distance allows for more accurate resource allocation in a heterogeneous cellular network. This is because it takes into account the actual distance between the transmitter and receiver, including the vertical distance. This can help optimize resource allocation, avoiding overloading certain cells with higher power signals, and reducing interference.
3) Enhanced User Experience: Using three-dimensional distance can improve the user experience by providing more accurate signal strength and coverage estimation. This is particularly important in a heterogeneous network where different cell types have different coverage areas and transmission power levels.

Overall, using three-dimensional distance in a heterogeneous cellular network provides more accurate path loss estimation, improved resource allocation and enhanced user experience. This leads to better network performance and a more reliable and efficient cellular network.

### A. CONTRIBUTIONS

The main contributions of this work are:

- Because new networks are always designed to be compatible with already implemented networks to minimise the loss of investment, single tier seems to be an impractical strategy in [28] and [30]. So, the 5G network in practice is a heterogeneous network that has been taken into account in our research.
- The researchers in [27] have taken into account single-user and free space path loss models in addition to multi-tier networks. Instantaneous power has been used to calculate SINR.
- It is demonstrated in [27], [28], and [30] that the PBS's antenna height (HP) can be lowered to obtain optimal coverage, however, this is impractical due to several difficulties, including vandalism and security.
- According to the researchers in [28] and [30], ASE crashes after base station densities of 1000.
- This work overcomes the pico BSs antenna height (HP) minimization issue raised in [27], [28], and [30].
- Similar to this, the issue of an ASE crash after a base station density of 1000 has been resolved in this study.
- This study demonstrates that greater coverage may be attained than with [27] by utilising the multi-slope 3GPP PL model and placing directional antennas at macro BSs.
- In this study, authors increased coverage by 10% over that in the [27].
- Authors in this paper increased ASE 2.5 times more than in the [27].
- The authors of this work used the multi-tier 3GPP PL model to take into account real-world scenarios and calculated SINR using average power.

## III. SYSTEM MODEL

A two-tier heterogeneous cellular network (HCN) system model shown in Figure 1 is a cellular network architecture that consists of two tiers of base stations (BSs) with different coverage areas and transmission power levels. The two tiers are macrocells and picocells. Macrocells are large coverage area base stations that provide coverage over a wide area. These base stations are typically used in rural areas and provide coverage for a large number of users. picocells are small coverage area base stations that provide coverage over a smaller area. These base stations are typically used in urban areas, where there are a large number of users in a small area. The two tiers of base stations are designed to work together to provide seamless connectivity and efficient resource allocation for different types of users as shown in Figure 1. The macrocells provide coverage over a wide area, while small cells provide coverage in areas where macrocells cannot reach or where the user density is high. This leads to better network performance, enhanced user experience, and improved resource allocation in a heterogeneous cellular network. The system model shown in Figure 1 is

a two-tier HCN that includes macrocell BSs (MBS), picocell BSs (PBS), and User Equipment (UE) which are the devices used by users to connect to the network and Backhaul (This is the link that connects the base stations to the main network and offers connectivity for data transmission and voice calls). Figure. 1 depicts a two-tier HCN model with MBSs and PBSs. The uniform distribution is applied on BSs and their nodes are distributed by Poisson point processes PPPs $\Phi_a$ having the BSs per unit area $\lambda_a$ with powers $P_a$ where $a = m$ for macro tier and $a = p$ for pico tier. Distribution on tier $m$ and tier $p$ are added to form combined distribution denoted by $\Phi_t$ with total BSs per unit area$\lambda_t$ which is given as $\lambda_t = \lambda_m + \lambda_p$. This is noticeable that the power of pico BSs $P_p$ is smaller than the power of macro BSs $P_m$, comparatively. The MBSs have a large coverage area due to their large power; On the other hand, PBSs have a smaller coverage area due to their small power. Consequently, the density of macro BS is smaller than the density of pico BS, i.e., $\lambda_m < \lambda_p$. The ratio $\lambda_p/\lambda_m = \beta$ which varies according to the Table. 2. The impact on network performance is analysed as a function of $\beta$. The system model has two different types of BSs having different powers, a limited number of user equipment and a multi-slope 3GPP PL model.

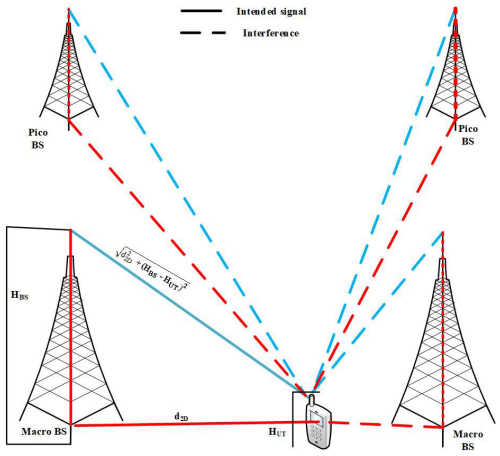


**FIGURE 1.** Two-tier HCN includes macrocell BSs, picocell BSs, User Equipment (UE).

The user equipment (UE) is assumed to be at the coordinate axis origin (0, 0) in Figure 1, which shows the system with MBSs and PBSs. Users will be allowed to connect using either macro or pico to any BS of any tier as long as they match the set specifications for average receive power. In this study, the user is connected to the same BS in both the uplink transmission and the downlink transmission, which is known as coupling association. As a result, the actions listed below and shown in flowchart 2 must be followed for the user to connect to the BS of any tier:

(1) The user's maximum average power received by all MBSs of m-tier $\Phi_1$ is calculated and then among all calculated received average power the strongest one is selected from $\Phi_1$.
(2) In the same way, the user's maximum average power received by all PBSs of p-tier $\Phi_2$ is calculated and then among all calculated received average power the strongest one is selected from $\Phi_2$.
(3) If the strongest average received power from m-tier is greater than the strongest average received power from p-tier, the user will connect with MBS; otherwise, with pico BS.

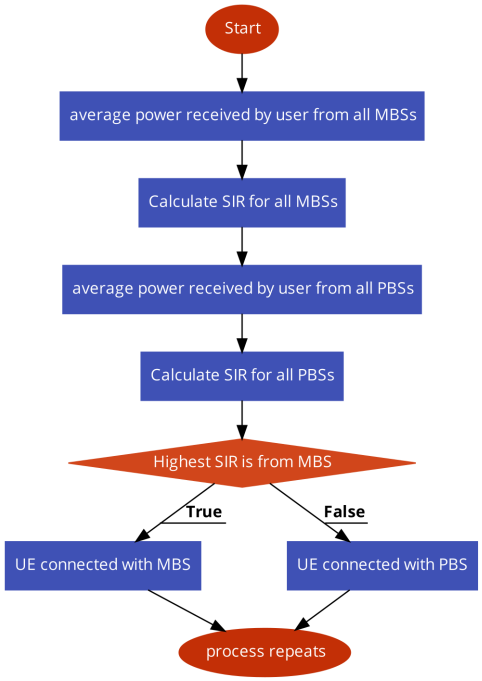


**FIGURE 2.** Flowchart shows steps that follow by BSs to connect with UE.

The Figure. 1 represents the system model, in which a user is connected with an MBS and receives interference signals from all other MBSs and PBSs of the network. The solid line in Figure 1 is the intended signal and dashed lines are interference signals. In most of the research work, users were assumed to be infinite, so that no BS in the network become empty and at least one user must be connected with a BS. However, it is practically not possible due to the limited power of BSs. Therefore, in our model by considering the finite number of users per BS, several BSs might serve no user and those BSs do not contribute in terms of interference power. The algorithm for connecting a UE with a BS of either tier is shown in Figure 2. Figure III shows the Path loss considering the distance of users from macro BSs which is calculated as per [31] and is given below:

$$PL = \max(PL_{LOS}, PL_{nLOS}),$$

$$PL_{LOS} = \begin{cases} PL_1 & 10m \le d_{2D} \le d'_{BP} \\ PL_2 & d'_{BP} \le d_{2D} \le 5km \end{cases}$$

$$PL_1 = 28.0 + \alpha M1LOS \times 10\log_{10} d_{3D} + 20\log_{10} f_c$$

$$PL_2 = 28.0 + \alpha M2LOS \times 10\log_{10} d_{3D} + 20\log_{10} f_c - 9\log_{10}[(d'_{BP})^2 + (H_{BS} - H_{UT})^2]$$

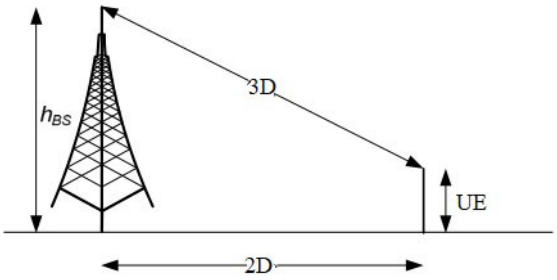


**FIGURE 3.** Scenario for calculating PL model.

$$PL_{nLOS} = 13.54 + \alpha MnLOS \times 10\log_{10} d_{3D} + 20\log_{10}(f_c) - 0.6(H_{UT} - 1.5)$$

Similarly, path loss considering the distance of users from pico BSs, which is calculated as per [31] and is given below:

$$PL = \max(PL_{LOS}, PL_{nLOS}),$$

$$PL_{LOS} = \begin{cases} PL_1 & 10m \le d_{2D} \le d'_{BP} \\ PL_2 & d'_{BP} \le d_{2D} \le 5km \end{cases}$$

$$PL_1 = 32.4 + \alpha P1LOS \times 10\log_{10}(d_{3D}) + 20\log_{10}(f_c)$$

$$PL_2 = 32.4 + \alpha P2LOS \times 10\log_{10}(d_{3D}) + 20\log_{10}(f_c) - 9.5\log_{10}[(d'_{BP})^2 + (H_{BS} - H_{UT})^2)]$$

$$PL_{nLOS} = 22.4 + \alpha PnLOS \times 10\log_{10}(d_{3D}) + 20\log_{10}(f_c) - 0.3(H_{UT} - 1.5)$$

where

$$d'_{BP} = 4H'_{BS}H'_{UT}\frac{f_c}{c} \tag{1}$$

where $f_c$ is given in Hz, it is the centre frequency normalized by $10^9$Hz, all distance-related values are normalized by 1m, $c = 3 \times 10^8$m/s is the speed of electromagnetic waves, the effective antenna height at the BS is represented by $H'_{BS}$ and $H'_{UT}$ represents the effective antenna height at UE. The $H'_{BS}$ and $H'_{UT}$ are computed as follows:

$$H'_{BS} = H_{BS} - H_E \tag{2}$$

$$H'_{UT} = H_{UT} - H_E \tag{3}$$

here $H_{BS}$ and $H_{UT}$ are the actual antenna heights, and $H_E$ is the effective environment height equal to 1m.

## IV. PERFORMANCE METRICS

The coverage, ASE and data rate are the basic performance parameters of an HCN [12], [26], [27]. The signal-to-Interference plus Noise Ratio (*SINR*) above the specified threshold $\chi$ is the coverage of the UE located at the origin. Mathematically given as

$$Pr[SINR > \chi] \tag{4}$$

and SINR in (4) is given as

$$SINR = \frac{I_s}{i_T + N_0} \tag{5}$$

In (5) $I_s$ is for the planned average power that a user intends to get from its linked BS, and $i_T$ stands for the overall interference received. Thermal noise, the Boltzmann constant, room temperature, and bandwidth are each represented by the symbols $N0 = KTB = -104$ dBm, $K$, $T$, and $B$. Because noise $N_0$ is so little and is provided by, SINR is truly SIR.

$$SIR = \frac{P_k G_k H_{k,i} D_{k,i}^{-\alpha}}{\sum_{i:b_i \in \Phi_t \setminus b_0} P_k g_k h_{k,i} d_{k,i}^{-\alpha}} \tag{6}$$

In (6) the numerator displays the product of the associated user's power, gain, Rayleigh distributed small-scale fading, and 3D distance from its serving BS, $b_0$, which is the *ith* BS of the *kth* tier. The denominator, in a similar manner, displays the overall interference at the user from all BSs of the network, with the exception of the $b_0$ and deactivated BSs as a result of IMC. Remember that deactivated BSs are in idle state and do not contribute any interference owing to IMC mode. The distance between the user and BS is three-dimensional (3D) and is given by (7) [31]

$$3D = \sqrt{2D^2 + (H_{BS} - H_{UT})^2}. \tag{7}$$

Area spectral efficiency (ASE) for a given randomly situated user is another performance criterion for an HCN. It is calculated as the sum of the highest average data rates per unit bandwidth ($BW$) per unit area supported by a cell's BS. The unit taken into consideration for ASE in this study is bps/Hz/Km$^2$. A system model's ASE in this study can be written as described in (8)

$$ASE = \sum_{k=1}^{2} \lambda_k SE_k \tag{8}$$

where (9) defines $SE_k$ as the spectral efficiency of the *kth* tier.

$$SE_k = \log_2(1 + SIR_k) \tag{9}$$

Data Rate is one of the major commercial performance metrics for HCN, which is calculated as

$$DataRate_k = \frac{BW}{Load}\log_2(1 + SIR_k) \tag{10}$$

In (10) BW is the bandwidth and load is the average load on the network.

## V. RESULTS AND DISCUSSION

### A. SIMULTAION TOOL

In this research paper, MATLAB is used to simulate heterogeneous cellular networks (HetNets) depicted in Figure 1 using the steps defined below:

1) Authors have defined the location of the macrocells, picocells, and user equipment (UE) in the simulation environment by using built-in functions poissrnd and rand.
2) Then creates a traffic generator to model the user behaviour and simulate the traffic load on the HetNet.
3) Then configured the network parameters using table 1.

4) Then calculates the path loss between the UE and each base station using a propagation model as defined in III.
5) Then models the interference caused by the co-channel and adjacent-channel cells
6) Finally simulate the system model as depicted in Figure 1 using the configured parameters and analyze the performance metrics such as signal-to-interference-plus-noise ratio (SINR), coverage, ASE and Data Rate.

Table 1 lists the design parameters together with their values and units for obtaining the findings. This section discusses the findings for coverage, ASE, and average data rate as functions of ($\beta$) when using various heights and gains of MBSs and PBSs antennas, referred to as HM, HP and GM, GP, respectively.

**TABLE 1. Simulation parameters.**

| Parameters | Values with units |
|---|---|
| Pico to Macro BS density ratio ($\beta$) | $\{10, 15, 30, 50, 65, 80, 333, 500, 1000, 1500, 2500\}$ [27] |
| Pico BS density ($\lambda_p$) | $\{0.1, 1, 10, 50, 65.065, 100, 500, 1000, 2500, 5000, \}$ 10000 (BSs/km$^2$) [27] |
| Tier BSs Power (TM, TP) | $\{46, 24\}$ dBm [27] |
| Gain of MBs ($minGM, maxGM$) | $\{0, 15\}$ dB [27] |
| Gain of PBSs ($minGP, maxGP$) | $\{0, 5\}$ dB [27] |
| Gain of UE antenna | 0 dB [27] |
| $min\|HM\|, max\|HM\|$ | $\{0, 23.5\}$ m [31] |
| $min\|HP\|, max\|HP\|$ | $\{0, 8.5\}$ m [31] |
| PL slopes for MBS [$\alpha$M1LOS, $\alpha$M2LOS, $\alpha$MnLOS] | $\{2.2, 4, 3.908\}$ [31] |
| PL slopes for PBS [$\alpha$P1LOS, $\alpha$P2LOS, $\alpha$PnLOS] | $\{2.1, 4, 3.53\}$ [31] |
| Carrier Frequency ($f_c$) | 2 GHz [31] |
| Bandwidth ($BW$) | 10 MHz [31] |
| Thermal Noise ($N_o$) | -104 dBm [31] |

## B. COVERAGE

For the system model illustrated in Figure 1 the probability of coverage is obtained by using parameters in Table 1. According to Figures 4 and Figure 5, the results for coverage with and without IMC have been achieved at *chi* equal to 0 dB for various HM and HP as a function of $\beta$ varies from 10 to 2500. The $\frac{\lambda_p}{\lambda_m} = \beta$ has been calculated in accordance with the [27] in Table 2.

### 1) ANTENNAS HEIGHT IMPACT ON COVERAGE

The results in Figure 4 were obtained utilising various heights for MBSs and PBSs antennas, HM and HP, respectively. For practical receivers, authors have considered SIR's minimum threshold $\chi = 0$ dB. It should be noted that the HM is 0.025 km, HP is 0.01 km and the height of user equipment (HU) is 0.0015 km [31]. However, $|HM|$, $|HP|$ and $|HU|$ are considered as the absolute difference between the antenna's actual height and user equipment height. Thus, $|HM|$ is 0.025 km – 0.0015 km which equals to be 0.0235 km. Similarly, $|HP|$ is 0.01 km – 0.0015 km and is equal to 0.0085 km. It should be noted in Figure 4 that authors have

**TABLE 2. Generations as per BSs density ratio ($\beta$) [27].**

| | |
|---|---|
| $\frac{\lambda_p}{\lambda_m} = \beta$ | Cellular Generations |
| $\frac{\lambda_p}{\lambda_m} \leq 10$ | $2^{nd}$ Generation $\sim 3^{rd}$ Generation |
| $10 < \frac{\lambda_p}{\lambda_m} < 60$ | $4^{th}$ Generation |
| $60 < \frac{\lambda_p}{\lambda_m} < 2500$ | $5^{th}$ Generation |
| $\frac{\lambda_p}{\lambda_m} > 2500$ | Ultradense Network (UDN)-(Beyond 5G) |

considered four cases with respect to the height of MBS and PBS antennas. Case-1 is shown with black colour and 0 marker having max $|HM| = 0.0235$ km and max $|HP| = 0.0085$ km. Case-2 is shown with green colour and $\diamond$ marker having values as max $|HM| = 0.0235$ km and min $|HP| = 0$ km. Case-3 is shown with red colour and $\times$ marker having min $|HM| = 0$ km and max $|HP| = 0.0085$ km. Case-4 is shown with blue colour and $\square$ marker having min $|HM| = 0$ km and min $|HP| = 0$ km.

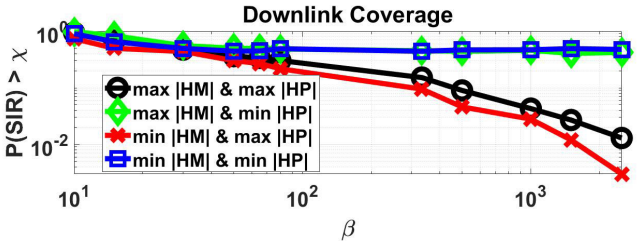


**FIGURE 4. Effect of antenna heights on Probability of Coverage without using IMC mode versus $\beta$.**

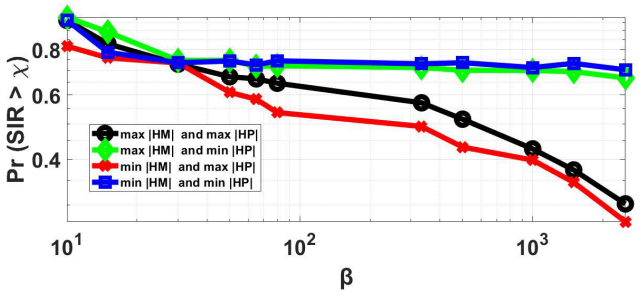


**FIGURE 5. Effect of antenna heights on Probability of Coverage using IMC mode versus $\beta$.**

Figure 6 shows dotted lines for the association of users with pico BSs and solid lines show the association of users with macro BSs. In Figure 4 the results of coverage have been obtained without using IMC mode where as the coverage results shown in Figure 5 are acquired by using IMC mode. From both the Figures, it is fairly evident that coverage results with IMC mode in Figure 5 have a considerable effect on the probability of coverage that is the coverage has improved than the coverage results found in Figure 4. IMC improves coverage probability because it allows the user equipment (UE) to remain connected to the network even when it is

not actively transmitting or receiving data. In cellular networks, UE typically alternate between active and idle modes. In active mode, the UE is connected to the network and is actively transmitting or receiving data. In idle mode, the UE is still connected to the network, but it is not actively transmitting or receiving data. When UE are in idle mode, they can still receive paging messages from the network. This allows the network to notify the UE when there is data available for it to receive. By having idle mode capability, UE can remain connected to the network for longer periods of time, which can increase the probability of successful communication between the UE and the network. Therefore, IMC has improved by 22% coverage probability by allowing UE to remain connected to the network for longer periods of time, even when they are not actively transmitting or receiving data.

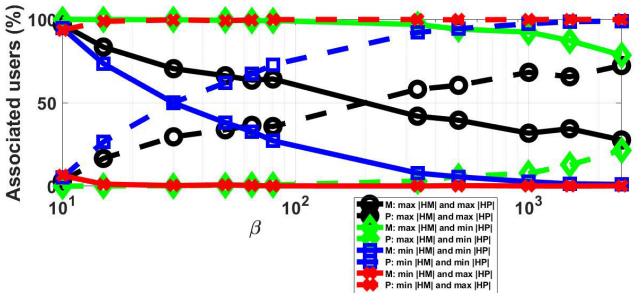


**FIGURE 6.** UEs Association to MBS and PBS using different Heights of MBS and PBS antennas versus $\beta$.

Figure 5 shows four cases with different colours. Each colour represents a different combination of antenna heights at MBSs and PBSs. For 5G we have $\beta > 60$ and results have been compared for this $\beta$ value. When MBS and PBS antennas are at their highest heights (max $|HM|$ and max $|HP|$) shown with black colour and 0 marker. In this condition, the probability of coverage is continuously decreasing. When MBS's and PBS's antennas are at their lowest and highest heights, respectively, this is shown in red colour and $\times$ marker (min $|HM|$ and max $|HP|$); in this situation, the probability of coverage also continually declines. The probability of the coverage staying steady state when MBS's antenna is at its maximum height and PBS's antenna is at its minimum height, as indicated by the green colour and $\diamond$ marker (max $|HM|$ and min $|HP|$). When both MBS and PBS antennas are at their lowest heights, this is shown by the colour blue and $\square$ marker (minimum $|HM|$ and minimum $|HP|$); in this case, the probability of coverage also stays constant until *beta* $>$ 60. The association of users with MBSs and PBSs depicted in Figure 6 is the reason for this. In the first scenario, when $|HM|$ and $|HP|$ are at their highest levels, users are first associated with MBSs before being offloaded to PBSs. However, because there are so many PBSs, there is a rise in interference, which lowers the probability of coverage. Users are connected to PBSs in the second scenario, when $|HM|$ and $|HP|$ are at their lowest and highest values, respectively. As *beta* grows, so does the number of PBSs, which increases interference and decreases the probability of coverage. Users are connected to MBSs in the third scenario, in which $|HM|$ is at its highest and $|HP|$ is at its lowest, and the probability of coverage remains in a steady state. This is caused by the high MBS power and low PBS power. PBSs consequently lost their advantage in interference. In the fourth case scenario, the majority of users are connected to MBSs when $|HM|$ and $|HP|$ are at their lowest levels, and as $\beta$ grows, all users are offloading from MBSs to PBSs. The coverage probability so continues to be steady state. This is due to the fact that, even when the interference caused by BSs that are relatively far away is taken into account, the signal power will start to lose out to the interference power as $\lambda_t$ goes to infinity. Overall, higher antennas can offer better coverage since they have a wider line of sight and can be pointed farther away, creating larger cells with less interference. This can be especially helpful for MBSs, which are frequently set up to cover a big area. In contrast, lower antennas, such as those used for PBSs, can provide more targeted coverage and can reduce the impact of interference from other cells. This can result in improved capacity and higher data rates for users in their coverage area. Hence, the lower height of the PBSs antenna provides better coverage depicted with green colour $\diamond$ marker and blue colour $\square$ marker in Figure 5. In this paper we have 10% improved coverage probability than [27] with all four cases.

### 2) ANTENNAS GAIN IMPACT ON COVERAGE

Antenna gain refers to the increase in signal strength that an antenna provides compared to an isotropic radiator, and it is measured in decibels (dB). The higher the gain of an antenna, the more focused and directional the signal will be, providing improved signal quality and coverage in specific directions. When it was noticed that antenna heights had an effect on the probability of coverage, the gains were taken to be 0 dB. According to the results presented in Figure 5, the probability of coverage is optimum when $|HP|$ is zero km, however, $|HM|$ does not matter whether it is minimum at zero km or maximum at 0.0235 km (case 3 and case 4). Nevertheless, it is practically impossible to make the antenna height ($|HM|$, $|HP|$) equal to zero due to vandalism and security concerns. Also, as demonstrated in Figure 7, authors found no influence of gain on the minimum $|HM| = 0$ km and minimum $|HP| = 0$ km, as well as the maximum $|HM| =$ 0.0235 km and minimum $|HP| = 0$ km as shown in Figure 8. As a result, authors have further researched the impact of the gain on a real-world scenario that involves the maximum $|HM|$ and $|HP|$. Results for MBS and PBS antennas have different gain values, as illustrated in Figure 9. The authors took four distinct gain values into consideration while creating Figure 9. Case 1 is max GM = 15 dB and max GP = 5 dB which is shown with black colour and zero 0 marker. Case 2 is max GM = 15 dB and min GP = 0 dB as depicted with green colour and $\Diamond$ marker. Case 3 is min GM = 0 dB and max

GP = 5 dB as indicated with red colour and × marker. Case 4 is min GM = 0 dB and min GP = 0 dB as appeared with blue colour and □ marker.

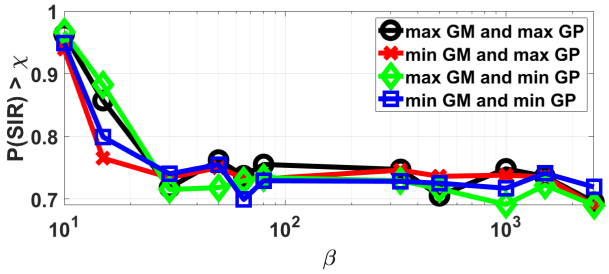


**FIGURE 7.** Effect of gains on Probability of coverage by considering min HM and min HP versus $\beta$.

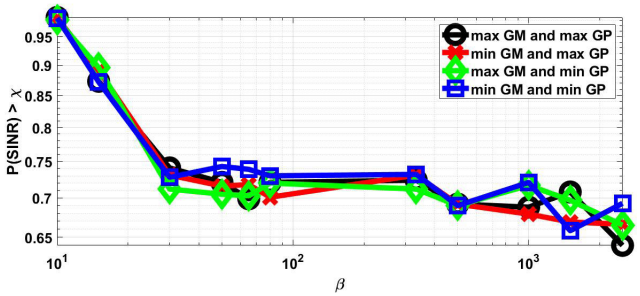


**FIGURE 8.** Effect of gains on Probability of coverage by considering min HP versus $\beta$.

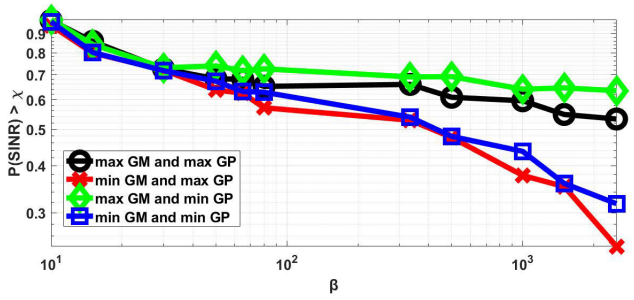


**FIGURE 9.** Effect of gains on Probability of coverage by considering max HM and max HP versus $\beta$.

Figure 9 shows the effect of gain with the practical case that is max $|HM|$ and max $|HP|$. It is observed from Figure 9 that coverage is maximum with green colour having max $GM = 15$ dB and min $GP = 0$ dB. This is because of the reduction in interference from MBS antennas due to their directivity. The black colour results shown in Figure 5 are the same as the blue colour results in Figure 9. On comparing the results of both the cases in Figure 9, the improvement in coverage with max GM and min GP as compared to min GM and min GP is approximately 32%. In [27] authors have analysed the maximum coverage with min $|HP|$ and they had seen no effect of gain on the probability of coverage. In this research authors have approximately 22% better coverage than [27] with a practical case that is max $|HM|$ and max $|HP|$ by applying gain on MBS antennas. Figure 9 shows that higher antenna gain can provide improved coverage and signal quality, as the signal is more focused and directional. This can be particularly useful for MBSs, which are typically deployed to provide coverage to a large area. In contrast, lower gain antennas, such as those used for PBSs, can provide more omnidirectional coverage and can reduce the impact of interference from other cells. This can result in improved capacity and higher data rates for users in their coverage area. However, lower gain antennas can also lead to reduced signal strength and coverage, as the signal is less focused and directional.

### C. ASE

The highest data rate attained for a randomly positioned UE in terms of bandwidth and area measured in bits per second per square metre (bps/Hz/m$^2$) is known as ASE. In this work, ASE has been calculated in bps/Hz/Km$^2$. The results of ASE have been obtained for the network model shown in Figure 1 under the simulation parameters shown in Table 1.

#### 1) ANTENNAS HEIGHT IMPACT ON ASE

In Figure 10, four cases representing the results of the study on the effect of heights on ASE are presented. All four cases shown with black 0 marker, green ◊ marker, red × marker and blue □ marker represents max $|HM|$ max $|HP|$, max $|HM|$ min $|HP|$, min $|HM|$ max $|HP|$ and min $|HM|$ min $|HP|$ respectively. It can be observed from the results represented with blue colour and □ marker in Figure 10 have maximum ASE. But, in reality, that is not feasible due to the minimum height of both antennas. Antennas that are placed higher can cover a larger area, which can result in fewer cells being needed to cover a given area, reducing the complexity of the network and potentially increasing ASE. However, increasing the height of the antenna also increases the distance between the antenna and the user device, which can result in a weaker signal and lower signal-to-interference ratio (SIR). This can reduce the overall performance of the network and decrease ASE represented with black colour and 0 marker in Figure 10. ASE with green colour and ◊ marker represents 2.5 times the higher value as compared to results in [27]. This is because of the realistic multi-slope path loss model considered in this research.

#### 2) ANTENNAS GAIN IMPACT ON ASE

By taking into account the GM = GP as having unity gain (0 dB), the impact of antenna heights on ASE was determined. According to those findings, ASE is maximum with minimum $|HM|$ and minimum $|HP|$, as illustrated in Figure 10. As a result, by taking into account four scenarios, writers of a min $|HM|$ and min $|HP|$ have further explored the effects of gains over it. Case-1 is shown with blue colour and □ marker which has min GM = 0 dB and min GP = 0 dB, case-2 is depicted with green colour, ◊ marker and has max

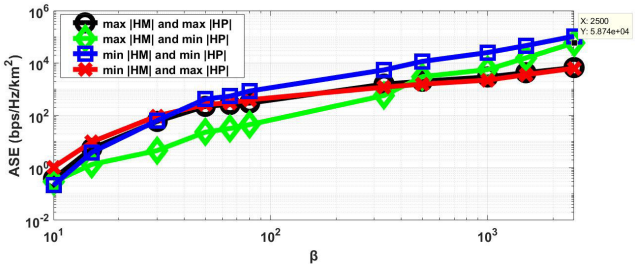


**FIGURE 10.** Effect of MBSs and PBSs antenna height on ASE versus $\beta$.

GM = 15 dB and min GP = 0 dB, case-3 is highlighted with red colour and × marker which has min GM = 0 dB and max GP = 5 dB and case-4 is represented with black colour and zero 0 marker which has max GM = 15 dB and max GP = 5 dB. Figure 11 displays the data together with the influence of gains on ASE. Because the antennas at both tiers (macro and pico) are mounted at the user's height, it can be seen that gain has no effect on ASE. The improvement of ASE with maximum $|HM|$ and minimum $|HP|$ is also demonstrated in Figure 10, therefore utilising these antenna heights the influence of gains is further examined. It can be observed from Figure 12 that by using directional antennas at pico BSs, ASE can be improved. Moreover, the effect of gain with max $|HM|$ and max $|HP|$ is shown in Figure 13. It can be observed from Figure 13 that by applying gain ASE reduces as compared to previous cases. Theoretically, it is explained by (8) where by using directional antennas at any BS of any tier, $\lambda$ reduces which is why ASE reduces. For the three cases as discussed above ASE improves rather than crashes.

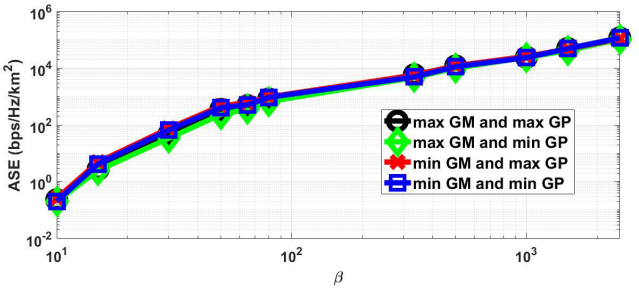


**FIGURE 11.** Effect of gain on ASE using min HM and min HP versus $\beta$.

### D. AVERAGE DATA RATE

Figure15 shows the average data rate in Mbps for the network shown in Figure 1. The data rate is directly proportional to the spectral efficiency (SE) as evident by (10). How efficiently bandwidth is utilized is termed spectral efficiency (SE). SE is measured in bps/Hz in this work. 6subsubsectionANTENNAS HEIGHT IMPACT ON AVERAGE DATA RATE It is observed that the height of the antenna has a major role in the data rate. Simulation results in Figure 15 show that when $|HM|$ is maximum and $|HP|$ is minimum as indicated by the green colour and ◊ marker, the overall average data rate is maximum. However, the average data rate

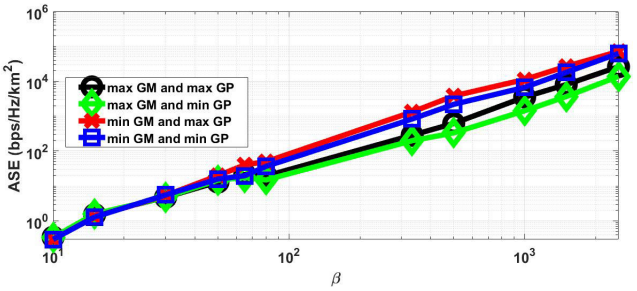


**FIGURE 12.** Effect of gain on ASE using max HM and min HP versus $\beta$.

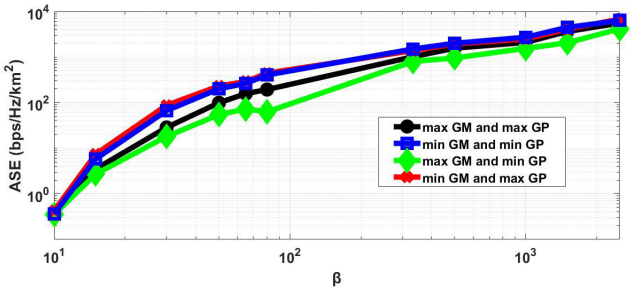


**FIGURE 13.** Effect of gain on ASE using max HM and max HP versus $\beta$.

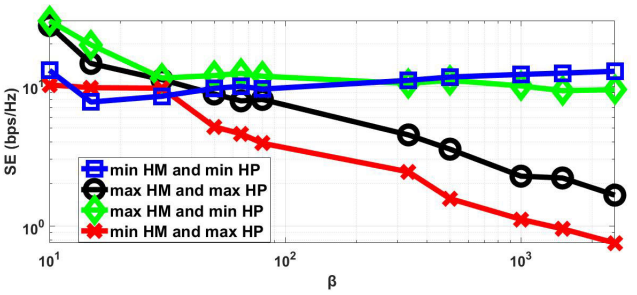


**FIGURE 14.** SE with different heights as a function of $\beta$.

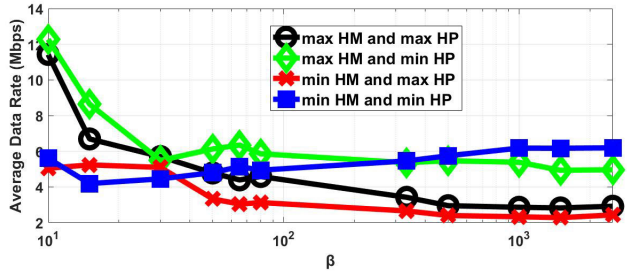


**FIGURE 15.** Effect of MBSs and PBSs antenna height on Avg data rate versus $\beta$.

reduces as $\beta$ increases due to the reduction in SE as shown in Figure 14.

#### 1) ANTENNAS GAIN IMPACT ON AVERAGE DATA RATE

In this subsection, the effect of gain by considering max HM and max HP on data rate as shown in Figure 16 is depicted.

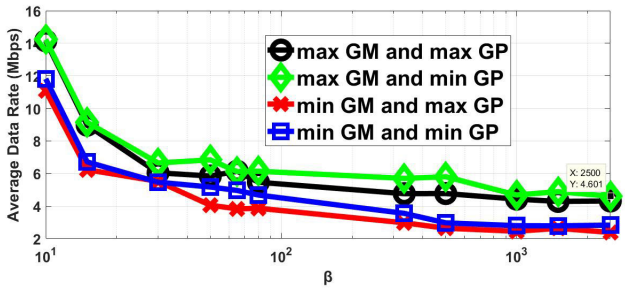


**FIGURE 16.** Effect of gain on data rate with max HM and max HP as a function of $\beta$.

It is observed that by applying gain on MBSs antenna the achieved data rate is as high as in max $|HM|$ and min $|HP|$ case without gain [27]. Simulation results in Figure 16 imply that to achieve a high data rate with max $|HM|$ and max $|HP|$ case, a directional antenna must be installed at macro BSs. Theoretically, (8) shows that by decreasing $\lambda_t$ SE increases. As $\lambda_m$ is decreased by using directional antennas at macro BSs which increase SE and also as per (10) by increasing SE, the data rate is also increased.

## VI. CONCLUSION

This work is on a network that has two types of BSs with respect to the power while using the IMC mode. The effect of height and gain of antennas as a function of $\beta$ has been observed. It is discovered that changing the heights and gains of the antenna while changing the connectivity of UEs impacts the coverage. According to earlier research on 5G and beyond networks, improved performance can be obtained by taking into account the pico BS's $|HP| = 0$ minimum antenna height, whereas gain has no influence on the probability of coverage. However, practically it is difficult due to security, vandalism and other issues. In this research, this issue is resolved along with improvement in coverage, ASE and average data rate by applying gain on MBS antennas while antenna heights on both tiers are at maximum. Furthermore, as per available literature, by considering homogeneous 5G and beyond networks ASE crushes as BSs density increases. In this work, authors have resolved the issue of ASE crush while not compromising on the performance of the network in terms of coverage, ASE and data rate.

## LIST OF ABBREVIATIONS

This list describes abbreviations that are used within the body of the document

| | |
|---|---|
| $\lambda_m$ | density of Macro BSs. |
| $\lambda_p$ | density of Pico BSs. |
| $\lambda_{BSs}$ | density of BSs. |
| *BS* | Base Station. |
| *BW* | Bandwidth. |
| *CDMA* | Code division multiple access. |
| *EE* | Energy Efficiency. |
| *FDMA* | frequency division multiple access. |
| *GM* | Gain of Macro BS antenna. |
| *GP* | Gain of Pico BS antenna. |
| *2D* | Two-dimensional distance. |
| *HetNets* | Heterogenous Cellular Network. |
| *HCN* | Heterogenous Cellular Network. |
| *HM* | Height of Macro BS antenna. |
| *HP* | Height of Pico BS antenna. |
| *HPPP* | Homogeneous Poisson point process. |
| *IMC* | Idle Mode Capability. |
| *LoS* | line-of-sight. |
| *MBS* | Macro Base Station. |
| *MIMO* | Multiple Input Multiple Output. |
| *NLoS* | non line-of-sight. |
| *3D* | Three-dimensional distance. |
| *OFDMA* | Orthogonal frequency DMA. |
| *PBS* | Pico Base Station. |
| *PSK* | Phase Shift Keying. |
| *PPP* | Poisson point process. |
| *PL* | Pathloss. |
| *QAM* | Quadrature amplitude modulation. |
| *RATs* | Radio Access Technologies. |
| *RAN* | Radio Access Network. |
| *SNR* | Signal-to-noise ratio. |
| *SINR* | Signal-to-interference plus noise ratio. |
| *3GPP* | Third generation partnership projects. |
| *SBSs* | Small Cell Base Stations. |
| *SE* | Spectral Efficiency. |
| *TDMA* | Time Division Multiple Access. |
| *UDNs* | Ultra Dense Networks. |
| *UE* | User Equipment. |
| *4G* | Fourth generation. |
| *5G* | Fifth generation. |
| *ASK* | Amplitude Shift Keying. |
| *AMC* | Adaptive Modulation and Coding. |
| *ASE* | Area Spectral Efficiency. |
| $\beta$ | Ratio of density of Pico BSs to Macro BSs. |

## ACKNOWLEDGMENT

The authors extend their appreciation to Researchers Supporting Project number (RSPD2023R553), King Saud University, Riyadh, Saudi Arabia.

## REFERENCES

[1] X. Lin, "An overview of 5G advanced evolution in 3GPP release 18," *IEEE Commun. Standards Mag.*, vol. 6, no. 3, pp. 77–83, Sep. 2022.
[2] M. M. Rahman, F. Khatun, S. I. Sami, and A. Uzzaman, "The evolving roles and impacts of 5G enabled technologies in healthcare: The world epidemic COVID-19 issues," *Array*, vol. 14, Jul. 2022, Art. no. 100178.
[3] J. Rendon Schneir, J. Bradford, A. Ajibulu, K. Pearson, K. Konstantinou, H. Osman, and G. Zimmermann, "A business case for 5G services in an industrial sea port area," *Telecommun. Policy*, vol. 46, no. 3, Apr. 2022, Art. no. 102264.
[4] D. López-Pérez, M. Ding, H. Claussen, and A. H. Jafari, "Towards 1 Gbps/UE in cellular systems: Understanding ultra-dense small cell deployments," *IEEE Commun. Surveys Tuts.*, vol. 17, no. 4, pp. 2078–2101, 4th Quart., 2015.

[5] J. Du and C. Jiang, "Traffic offloading in heterogeneous networks," in *Cooperation and Integration in 6G Heterogeneous Networks*. Cham, Switzerland: Springer, 2023, pp. 17–44.
[6] X. Chu, D. Lopez-Perez, Y. Yang, and F. Gunnarsson, *Heterogeneous Cellular Networks: Theory, Simulation and Deployment*. Cambridge, U.K.: Cambridge Univ. Press, 2013.
[7] H.-S. Jo, Y. J. Sang, P. Xia, and J. G. Andrews, "Heterogeneous cellular networks with flexible cell association: A comprehensive downlink SINR analysis," *IEEE Trans. Wireless Commun.*, vol. 11, no. 10, pp. 3484–3495, Oct. 2012.
[8] J. Chen, P. Rauber, D. Singh, C. Sundarraman, P. Tinnakornsrisuphap, and M. Yavuz, "Femtocells—Architecture & network aspects," *Qualcomm*, vol. 28, pp. 1–7, Jan. 2010.
[9] M. Ghanbarisabagh, G. Vetharatnam, E. Giacoumidis, and S. Momeni Malayer, "Capacity improvement in 5G networks using femtocell," *Wireless Pers. Commun.*, vol. 105, no. 3, pp. 1027–1038, Apr. 2019.
[10] F. Baccelli and B. Błaszczyszyn, "Stochastic geometry and wireless networks: Volume II applications," *Found. Trends Netw.*, vol. 4, nos. 1–2, pp. 1–312, Jan. 2010.
[11] M. Haenggi, *Stochastic Geometry for Wireless Networks*. Cambridge, U.K.: Cambridge Univ. Press, 2012.
[12] D. Stoyan, W. S. Kendall, S. N. Chiu, and J. Mecke, *Stochastic Geometry and Its Applications*. Hoboken, NJ, USA: Wiley, 2013.
[13] Y. S. Soh, T. Q. S. Quek, M. Kountouris, and H. Shin, "Energy efficient heterogeneous cellular networks," *IEEE J. Sel. Areas Commun.*, vol. 31, no. 5, pp. 840–850, May 2013.
[14] Q. Ye, B. Rong, Y. Chen, M. Al-Shalash, C. Caramanis, and J. G. Andrews, "User association for load balancing in heterogeneous cellular networks," *IEEE Trans. Wireless Commun.*, vol. 12, no. 6, pp. 2706–2716, Jun. 2013.
[15] J. Yang, "Stochastic geometry based modeling and performance analysis of ultra-dense cellular networks," Ph.D. dissertation, Dept. Eng. Inf. Technol., Univ. Technol. Sydney, Sydney, NSW, Australia, 2019.
[16] M. Di Renzo, A. Guidotti, and G. E. Corazza, "Average rate of downlink heterogeneous cellular networks over generalized fading channels: A stochastic geometry approach," *IEEE Trans. Commun.*, vol. 61, no. 7, pp. 3050–3071, Jul. 2013.
[17] J. G. Andrews, F. Baccelli, and R. K. Ganti, "A tractable approach to coverage and rate in cellular networks," *IEEE Trans. Commun.*, vol. 59, no. 11, pp. 3122–3134, Oct. 2011.
[18] P. Swami and V. Bhatia, "Noma for 5G and beyond wireless networks," in *A Glimpse Beyond 5G in Wireless Networks*. Cham, Switzerland: Springer, 2023, pp. 143–166.
[19] X. Zhang and J. G. Andrews, "Downlink cellular network analysis with multi-slope path loss models," *IEEE Trans. Commun.*, vol. 63, no. 5, pp. 1881–1894, May 2015.
[20] M. Ding, P. Wang, and D. López-Pérez, "Performance impact of LoS and NLoS transmissions in dense cellular networks," *IEEE Trans. Wireless Commun.*, vol. 15, no. 3, pp. 2365–2380, Mar. 2016.
[21] A. AlAmmouri, J. G. Andrews, and F. Baccelli, "SINR and throughput of dense cellular networks with stretched exponential path loss," *IEEE Trans. Wireless Commun.*, vol. 17, no. 2, pp. 1147–1160, Feb. 2018.
[22] S. Lee and K. Huang, "Coverage and economy of cellular networks with many base stations," *IEEE Commun. Lett.*, vol. 16, no. 7, pp. 1038–1040, Jul. 2012.
[23] M. Di Renzo, W. Lu, and P. Guan, "The intensity matching approach: A tractable stochastic geometry approximation to system-level analysis of cellular networks," *IEEE Trans. Wireless Commun.*, vol. 15, no. 9, pp. 5963–5983, Sep. 2016.
[24] S. M. Yu and S.-L. Kim, "Downlink capacity and base station density in cellular networks," in *Proc. 11th Int. Symp. Workshops Model. Optim. Mobile, Ad Hoc Wireless Netw. (WiOpt)*, 2013, pp. 119–124.
[25] H. S. Dhillon, R. K. Ganti, F. Baccelli, and J. G. Andrews, "Modeling and analysis of K-tier downlink heterogeneous cellular networks," *IEEE J. Sel. Areas Commun.*, vol. 30, no. 3, pp. 550–560, Apr. 2012.
[26] M. Ding, D. L. Perez, G. Mao, and Z. Lin, "Study on the idle mode capability with LoS and NLoS transmissions," in *Proc. IEEE Global Commun. Conf. (GLOBECOM)*, Dec. 2016, pp. 1–6.
[27] A. Abbasi, M. M. Shaikh, S. A. Dahri, S. A. Soomro, and F. A. Panhwar, "Analysis of coverage and area spectral efficiency under various design parameters of heterogeneous cellular network," *Int. J. Electron. Telecommun.*, vol. 67, pp. 639–645, Nov. 2021.
[28] M. Ding and D. L. Perez, "Please lower small cell antenna heights in 5G," in *Proc. IEEE Global Commun. Conf. (GLOBECOM)*, Dec. 2016, pp. 1–6.
[29] M. Ding and D. López-Pérez, "Performance impact of base station antenna heights in dense cellular networks," *IEEE Trans. Wireless Commun.*, vol. 16, no. 12, pp. 8147–8161, Dec. 2017.
[30] A. H. Jafari, D. López-Pérez, M. Ding, and J. Zhang, "Performance analysis of dense small cell networks with practical antenna heights under Rician fading," *IEEE Access*, vol. 6, pp. 9960–9974, 2018.
[31] *Study on Channel Model for Frequencies From 0.5 to 100 GHz*, ETSI, 3rd Generation Partnership Project (3GPP), 2018, vol. 38.

**SAFIA AMIR DAHRI** received the B.E. and M.E. degrees from the Department of Electronic Engineering, Quaid-e-Awam University of Engineering, Science and Technology (QUEST), Nawabshah, Sindh, Pakistan, in 2011 and 2014, respectively, where she is currently pursuing the Ph.D. degree. She is an Assistant Professor with the Department of Telecommunication Engineering, QUEST. Her research interests include wireless communications with a special interest in heterogeneous cellular networks.

**MUHAMMAD MUJTABA SHAIKH** received the bachelor's degree in electronic engineering from the Mehran University of Engineering and Technology, Jamshoro, Sindh, Pakistan, in 2001, the M.S. degree from Usman Institute, Hamdard University, Karachi, Pakistan, in 2006, the Ph.D. degree in telecommunication engineering from the University of Malaga, Spain, in 2017. His Ph.D. thesis topic is "Heterogeneous Cellular Networks Under Diverse Coupling and Association Criteria." From 2003 to 2008, he was an Assistant Manager with the Communication and Scada Department, Karachi Electric Supply Corporation (KESC), Karachi. From 2014 to 2017, he was a Researcher with the Department of Communications Engineering, University of Malaga. Since 2008, he has been with the Department of Electronic Engineering, Quaid-e-Awam University of Engineering, Science and Technology, Nawabshah, Sindh, Pakistan, where he has been a Professor and the Head of the Telecommunication Engineering Department, since 2019. His main research interests include underwater sensor networks, small-cell networks, LTE-A, NOMA with mm-wave communication, 5G and 6G networks, and technologies with a special interest in heterogeneous cellular networks.

**MUSAED ALHUSSEIN** received the B.S. degree in computer engineering from King Saud University (KSU), Riyadh, Saudi Arabia, in 1988, and the M.S. and Ph.D. degrees in computer science and engineering from the University of South Florida, Tampa, FL, USA, in 1992 and 1997, respectively. He is a Professor with the Department of Computer Engineering, College of Computer and Information Sciences, KSU. Since 1997, he has been in the Faculty of the Computer Engineering Department, College of Computer and Information Science, KSU. Recently, he has been successful in winning a research project in the area of AI for healthcare, which is funded by the Ministry of Education, Saudi Arabia. He is the Founder and the Director of the Embedded Computing and Signal Processing Research (ECASP) Laboratory. His research interests include typical computer architecture and signal-processing topics with an emphasis on big data, machine/deep learning, VLSI testing and verification, embedded and pervasive computing, cyber-physical systems, mobile cloud computing, big data, e-healthcare, and body area networks.

**MUHAMMAD AFZAL SOOMRO** received the master's and Ph.D. degrees in mathematics from Quaid-i-Azam University, Islamabad, in 2007 and 2013, respectively. He is an Associate Professor with the Department of Mathematics and Statistics, Quaid-e-Awam University of Engineering Science and Technology (QUEST), Sindh, Pakistan. He has authored and coauthored more than 15 publications. His research interests include pure mathematics, geometry, and topology.

**KHURSHEED AURANGZEB** (Senior Member, IEEE) received the B.S. degree in computer engineering from the COMSATS Institute of Information Technology, Abbottabad, Pakistan, in 2006, the M.S. degree in electrical engineering (system-on-chip design) from Linkoping University, Sweden, in 2009, and the Ph.D. degree in electronics design from Mid Sweden University, Sweden, in June 2013. He is an Associate Professor with the Department of Computer Engineering, College of Computer and Information Sciences, King Saud University (KSU), Riyadh, Saudi Arabia. He has more than 15 years of excellent experience as an instructor and researcher in data analytics, machine/deep learning, signal processing, electronic circuits/systems, and embedded systems. He was involved in many research projects as a principal investigator and a co-principal investigator. He has authored and coauthored more than 90 publications, including IEEE/ACM/Springer/Hindawi/MDPI journals and flagship conference papers. His research interests include the diverse fields of embedded systems, computer architecture, signal processing, wireless sensor networks, communication, and camera-based sensor networks with an emphasis on big data and machine/deep learning with applications in smart grids, precision agriculture, and healthcare.

**MUHAMMAD IMRAN** (Member, IEEE) is a Senior Lecturer with the Institute of Innovation, Science and Sustainability, Federation University, Australia. He is the founding Leader of the Wireless Networks and Security (WINS) Research Group. He has completed many international collaborative research projects with reputable universities. He has published more than 300 research articles in peer-reviewed, highly reputable international conferences and journals. He is included in the 2022 Clarivate Highly Cited Researchers list in the category of computer science. His research interests include mobile and wireless networks, the Internet of Things, big data analytics, cloud/edge computing, and information security. He has been consecutively awarded Outstanding Associate Editor of *FGCS* and IEEE Access, in 2018, 2019, and 2021, respectively. He served as the Editor-in-Chief for *European Alliance for Innovation (EAI) Transactions on Pervasive Health and Technology* and an Associate Editor for *IEEE Communications Magazine*. He is serving as an Associate Editor for top-ranked international journals, such as IEEE Network, *Future Generation Computer Systems*, and IEEE Access.